Collaborative Control for a Robotic Wheelchair: Evaluation of Performance, Attention and Workload

Tom Carlson, *Member IEEE,* and Yiannis Demiris, *Senior Member IEEE*

Abstract—**Powered wheelchair users often struggle to drive safely and effectively and in more critical cases can only get around when accompanied by an assistant. To address these issues, we propose a collaborative control mechanism that assists the user as and when they require help. The system uses a multiple–hypotheses method to predict the driver's intentions and if necessary, adjusts the control signals to achieve the desired goal safely. The main emphasis of this paper is on a comprehensive evaluation, where we not only look at the system performance, but, perhaps more importantly, we characterise the user performance, in an experiment that combines eye–tracking with a secondary task. Without assistance, participants experienced multiple collisions whilst driving around the predefined route. Conversely, when they were assisted by the collaborative controller, not only did they drive more safely, but they were able to pay less attention to their driving, resulting in a reduced cognitive workload. We discuss the importance of these results and their implications for other applications of shared control, such as brain–machine interfaces, where it could be used to compensate for both the low frequency and the low resolution of the user input.**

I. INTRODUCTION

MANY people who suffer from mobility–impairments rely on powered wheelchairs to get out and about. In 2000, it was estimated that there were over 11350 electrically powered indoor/outdoor chair (EPIOC) users in the UK alone and this number was growing steadily by over 3500 per year [1]. However, a substantial number of users find it difficult to operate their chairs effectively [2]. In a study of young people using EPIOCs, Evans *et al.* found common accidents that occurred included "the chair running into people" and "banging into furniture" [3]. In another study, Frank *et al.* reported that over 10% of users had accidents within four months of receiving their EPIOC [4]. This shows that there is a clear need for the development of smart wheelchairs that would empower people with mobility impairments to get on safely with their activities of daily living.

Cooper *et al.* survey many components of wheelchair design: everything from mechanical aspects, interfaces and control algorithms to ISO standards that are being developed to assist users in driving safely [5]. However, in this paper we focus specifically on the evaluation of shared control methodologies. There are many approaches to assisted mobility, for example, Taha *et al.* [6] provide a high level of autonomation that requires relatively little user interaction and Zeng *et al.* [7] provide the possibility of guiding the user along trajectories that have previously been "walked–through". For people with severe physical disabilities that might prevent them from interacting through conventional interfaces, Millán *et al.* developed a brain machine interface [8], while Simpson and Levine have experimented with voice control [9]. Many hybrid systems, such as Wheelesley [10] and the NavChair [11] have also been developed, which can switch (sometimes autonomously) between different modes of operation. Ding and Cooper present a more comprehensive comparison of intelligent wheelchairs in their review paper [12].

The collaborative control methodology that we have proposed infers the user's intentions from their joystick input, based upon the affordances of the local environment [13]. In line with Nisbet's recommendations [14], the wheelchair only adjusts the motor control signals if the user requires assistance to complete the desired manoeuvre safely. However, whilst wheelchair users are driving, they are often concurrently interacting with their surroundings or other people. For example, Brandt *et al.* found that 87% of the 111 people surveyed used their wheelchairs to go shopping [15]. In this example, there is a clear need for divided attention between manoeuvring the wheelchair safely and searching for items on shelves. Consequently, traditional evaluation metrics from the field of robotics (e.g. speed and accuracy) are not sufficient to determine the success of a system in such circumstances. Instead, human factors should also be taken into account.

The primary contribution of this paper to the shared control literature is in terms of the comprehensive human factors analysis. We collectively examine the effects of collaborative control by employing: joystick signal analysis [16], secondary tasks [17] and eye-tracking [18], in addition to standard system performance metrics. An extensive study with 21 healthy participants and 1 wheelchair user yields statistically significant results that confirm that the findings from previous studies are both cumulative and repeatable over longer and more complex tasks. Moreover, a potential end-user of the system exhibits similar traits to the healthy subjects.

This paper begins by formalising our collaborative control architecture and explaining our choice of implementation. We then describe the experiments that we conducted with able–bodied users in an office environment. The results show that the collaborative controller enabled people to drive more safely, whilst concurrently reducing the demands on visual attention, cognitive workload and manual dexterity. We then compare these statistically significant results with those of a case study involving an experienced mobility–impaired

T. Carlson is jointly with the Defitech Chair in Non-Invasive Brain Machine Interface (CNBI), École Polytechnique Fédérale de Lausanne (EPFL), Station 11, 1015 Lausanne, Switzerland and the Department of Electrical and Electronic Engineering, Imperial College London, SW7 2AZ, UK, e-mail: tom.carlson@epfl.ch.

Y. Demiris is with the Department of Electrical and Electronic Engineering, Imperial College London, SW7 2AZ, UK, e-mail: y.demiris@imperial.ac.uk.
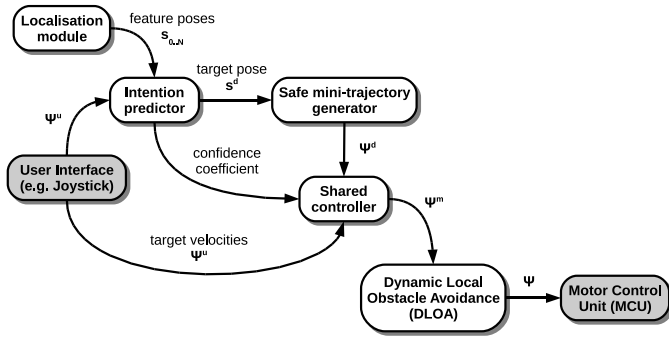
Fig. 1. The collaborative control architecture. The symbol $\boldsymbol{\Psi}$ indicates a translational and rotational velocity tuple, whereas $\mathbf{s}$ denotes an (x, y, θ) pose.

wheelchair user. In doing so, we find that even proficient wheelchair users can benefit from shared control under specific circumstances, e.g. when they are under a heightened workload, or are inattentive to the driving task.

II. COLLABORATIVE CONTROL

In contrast with discrete approaches to shared control, whereby a cognitively disabled user was able to indicate a *final destination*, to which the wheelchair would drive autonomously [19], we are focussed towards people with physical disabilities who can still use an analogue joystick input, to a certain extent. A more appropriate solution for this situation would be where the wheelchair autonomously follows a deliberative plan, with the user intervening as and when they wish to deviate from it [20]. However, as discussed in the Introduction, we wanted the user to be actively involved in the movement as much as possible. Therefore, our collaborative control system (Fig. 1) is designed to: determine the user's intention; verify the desired action is safe to perform and, where necessary, adjust the resultant control signals to achieve the goal safely. We define a safe action as one that does not result in a collision. If a crash is predicted, evasive action must be taken and this is provided by our dynamic local obstacle avoidance algorithm, which is described later in this section.

We extend the idea of *orientation correction*, where the heading of the wheelchair is constrained to fall within a certain error margin of a pre-selected goal [21], by introducing the concept of *safe mini-trajectories*. These are dynamically generated paths, which provide a safe passage from the current wheelchair position to a sub-goal (e.g. through a doorway) and primarily offer short term navigational assistance, rather than obstacle avoidance. For example they ensure that you approach a doorway from a suitable angle to pass through with relative ease. In addition, rather than pre-selecting a single target, we continuously update our prediction of the user's intentions, based upon both the globally pre–mapped and the locally perceived affordances of the surroundings. In this navigation task, the affordances are defined as areas that are navigable or places where the wheelchair should stop.

A. Notation

Here we define the notation that will be used throughout the following sections, when describing the individual components of the collaborative control system. The sampling period (T) is set to be $100\,\mathrm{ms}$, since we are sampling from our data acquisition module (DAQ), laser scanner and sonar sensors at $10\,\mathrm{Hz}$ on the actual wheelchair. Note that all angles are given in radians and will be constrained to lie on the interval $(-\pi, \pi)$. We will be using the symbol $\odot$ to denote the Hadamard product (i.e. the element–wise multiplication between two matrices of the same dimensions). On any variable, a superscript c relates to the properties of the actual wheelchair, superscript m indicates motor commands, superscript u denotes user input and superscript d denotes the desired state. For example, $\mathbf{s}_n^d$ denotes the n-th desired pose of the wheelchair, whereas $\mathbf{s}_n^c$ denotes what actually happened: the n-th physical pose of the wheelchair. Translational velocities are written as v and rotational velocities as ω. We define the following vector to hold the state information:

$$\mathbf{s} := \begin{bmatrix} x & y & \theta \end{bmatrix}^T, \tag{1}$$

and the input to the system is given as:

$$\boldsymbol{\Psi} := \begin{bmatrix} v & \omega \end{bmatrix}^T. \tag{2}$$

B. Localisation

In our experiments, the wheelchair was operating in a known, indoor, mapped environment, which, for example, would also be typical for a home–user, or a patient in a rehabilitation centre. Therefore we were able to use a reliable and inexpensive computer vision based localisation system, which determined the position of the wheelchair with respect to fiducials (fixed 2D paper markers) on the ceiling, as described in [13]. A camera was positioned on the wheelchair looking directly towards the ceiling, i.e. with its z-axis perpendicular to the plane of the fiducials. To overcome the extremes of brightness caused by the lighting, an adaptive Gaussian thresholding function was applied to the images. Once a fiducial had been detected in the camera's viewport, a transformation matrix was computed—based upon the position, size and orientation of the marker—that determined the cameras position relative to that specific marker [22]. Since, in our case, each fiducial's position was known in the global coordinate system and the relative placement of the camera on the wheelchair, we could determine the pose of the chair. In practice we were able to achieve a localisation accuracy within $5\,\mathrm{cm}$ and $2\,^\circ$ orientation.

In cases where it would be undesirable to place markers in the environment, approaches such as active localisation [23], or the widely studied methods of SLAM (simultaneous localisation and mapping) [24] could be used. As a compromise, in partially known environments, it may be desirable to fuse information from several different information sources, as was done in [19].

C. Prediction of Intent

There are many different approaches to intention prediction and plan recognition [25], [26]. We have chosen to perform the plan recognition using a multiple hypotheses method, following the approach we used in action recognition and imitation [27]. In this methodology, all the user's known
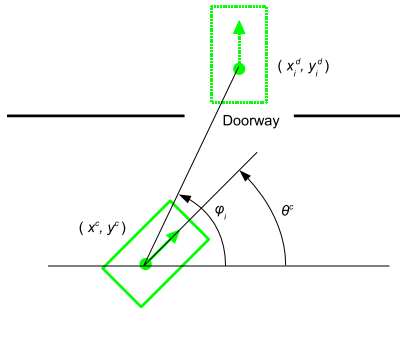
Fig. 2. Calculating the angle and Euclidean distance to the i-th desired target pose ("drive through doorway"), for the confidence coefficient.

actions are represented by inverse models. Between them, they predict in parallel the required states of the system to achieve each of these tasks. By comparing the actual state of the system with these predictions, we generate a *confidence* of each task being undertaken.

Our hypotheses are task based, so we manually define targets of interest, such as the poses of doorways and desks, which the user may wish to drive through or approach. For a practical application, these activities of daily living could be pre–defined by the end–user, a therapist or a family member, according to the user's needs.

The inverse model (Section II-E), which aims to minimise the distance to the target and angle between the heading of the wheelchair and the target, is instantiated for each of these targets. This then deterministically generates the possible next states of the wheelchair. In this experiment there were $N_T = 3$ pre-defined targets (each of the doorways in Fig. 6). This results in 3 known hypotheses of the potential tasks to be performed.

For each of the N_T hypotheses, we generate a confidence coefficient, C_i (Equation 3), which represents the confidence of that particular (i–th) prediction being correct. This coefficient is the product of two functions: the first (Equation 4) is computed using the Euclidean distance from the current wheelchair pose (s^c) to the i-th target (s_i^d), the second (Equation 6) is based upon the heading of the chair (θ^c), compared with the angle to the i-th target (ϕ_i, Equation 5), as shown in Fig. 2. The scaling factor (μ) in Equation 6 determines the sensitivity towards the angular error and was experimentally set to 2.0, which yielded satisfactory tolerance.

$$C_i = C_{e,i}C_{\theta,i}, \quad \text{where } i \in \{1, \ldots, N_T\}, \quad (3)$$

$$C_{e,i} = \exp\left\{-\sqrt{(x_i^d - x^c)^2 + (y_i^d - y^c)^2}\right\}, \quad (4)$$

$$\phi_i = \text{atan2}\left((y_i^d - y^c), (x_i^d - x^c)\right), \quad (5)$$

$$C_{\theta,i} = \exp\left\{-\frac{\mu}{\pi}|\theta^c - \phi_i|\right\}. \quad (6)$$

The exponential base functions in the confidence coefficient, mean that it falls off steeply as spatial or angular errors are introduced. The resultant function also has the desirable property of scaling the output so that it falls on the interval (0, 1], which makes it easy to compare competing hypotheses. However, we

also deal with the case that the user is not performing any of the known tasks. This is achieved by introducing a confidence threshold value, C_{thresh}, below which, no assistance is given. Once this threshold has been surpassed, we apply winner–takes–all to determine the user's intention.

If $C_{thresh} = 0$, the wheelchair would always be attracted to the most likely target. If $0 < C_{thresh} < 1$, there will be some occasions when the wheelchair is attracted to a likely target and some when the wheelchair will not be attracted to any target at all. If $C_{thresh} = 1$, the wheelchair will never be attracted to a target and the user will always have full control. When predicting the user's intended target, a lower value of C_{thresh} will increase the false positive rate, whereas a higher value will reduce the true positive rate. We experimentally set the confidence threshold C_{thresh} to be 0.2, which maximised the trade–off between the true–positive and false–positive rates of target detection, in the scenario described in [13]

Several hypotheses can be easily generated simply by storing the poses of interesting targets. In this set of experiments, we take the targets to be the locations of doorways in our pre-mapped environment (see Fig. 6). In an unknown environment, new targets could be added automatically as new features are incrementally added to the map [24].

D. Safe Mini–Trajectory

If a hypothesis is deemed to be correct by the intention predictor module, a path known as the safe mini–trajectory is planned from the current wheelchair pose s_n^c to the corresponding desired pose s_n^d. There are many approaches for solving this local path–planning problem, such as the VFH+ [28] and look ahead planners, like the dynamic window approach [29]. These approaches use dynamic simulations of the vehicle to plan ahead and will be revisited for local obstacle avoidance in Section II-H.

Similar trajectories can also be generated using geometric approaches, such as the elastic bands method [30]. We base our implementation on this method, where we iteratively insert waypoints into the path until there are no intersections between the bounding box of the wheelchair and any of the known map features [13]. We use the bounding box approximation to introduce a safety margin, since often the user's limbs do not all fall within the footprint of the wheelchair. Waypoints are also inserted perpendicular to the door opening, to ensure an appropriate approach trajectory. The path is then interpolated using B-splines to create a smooth trajectory. Whichever method is chosen, the resulting points (s_n^d) are then fed through an inverse model of the wheelchair, which generates appropriate controls signals to follow the safe mini-trajectory, should such a behaviour be required.

E. Wheelchair Inverse Model

An inverse model estimates the control signals that are required to move a system from its current state into a desired state and is akin to a controller [25]. In our case, this means determining the translational and rotational velocity commands required to move the wheelchair from its current pose (s_n^c) to the desired pose (s_n^d). In order to achieve this, we first

generate a path to the target location, as previously described in Section II-D.

Next we use a control law to move the wheelchair from one waypoint ($\mathbf{s}_n^c \approx \mathbf{s}_{n-1}^d$) to the next ($\mathbf{s}_n^d$) along the path. A variety of methods to do this—such as path following with orientation correction—are discussed in [31]. In our case, we re–formulate our problem in polar coordinates, as described in [32]. For the inverse model, we use the Euclidean distance (ρ_n) and angle (α_n) between the target position and the chair's current pose, in a similar manner to when we generate the confidence coefficient (Equation 3, Fig. 2). Therefore, the error signal vector is the difference between the target pose and the current wheelchair pose:

$$\mathbf{e}_n = \begin{bmatrix} e_{x,n} \\ e_{y,n} \\ e_{\theta,n} \end{bmatrix} = \mathbf{s}_n^d - \mathbf{s}_n^c, \tag{7}$$

$$\rho_n = \sqrt{(e_{x,n})^2 + (e_{y,n})^2}, \tag{8}$$

$$\alpha_n = \operatorname{atan2}(e_{y,n}, e_{x,n}) - \theta_n^c. \tag{9}$$

An additional angular component is introduced that aims to correct the final desired heading of the wheelchair:

$$\beta_n = \theta_n^d - \alpha_n. \tag{10}$$

The steady state error of the system is small, compared with the error in the wheelchair's sensory inputs. Therefore, since we are concerned more with stability, we will not consider the integral error component in our controller [33]. However, to prevent any overshoot, we add a derivative component to providing some damping in the control law described by [32]. This results in the following PD (proportional plus derivative) controller, which generates the components of the desired translational and rotational velocity tuple ($\boldsymbol{\Psi}_n^d$):

$$v_n^d = k_\rho \rho_n + k_{d\rho} \frac{\rho_n - \rho_{n-1}}{T}, \tag{11}$$

$$\omega_n^d = k_\alpha \alpha_n + k_\beta \beta_n + k_{d\alpha} \frac{\alpha_n - \alpha_{n-1}}{T} + k_{d\beta} \frac{\beta_n - \beta_{n-1}}{T}. \tag{12}$$

We set the parameters by experimentally increasing the proportional coefficients until there was a slight overshoot and then we introduced the derivative coefficients with the aim of critically damping the system. The parameters used in our experiments were:

$$\begin{aligned} k &= (k_\rho, k_\alpha, k_\beta, k_{d\rho}, k_{d\alpha}, k_{d\beta}) \\ &= (100, 180, -15, -5, 25, -0.1). \end{aligned} \tag{13}$$

F. Wheelchair Forward Model

We now introduce the concept of a forward model, which describes the predicted behaviour of the wheelchair. A forward model estimates the next state of the system, given the current state and current inputs [25]. So in our case, the state refers to the pose ($\mathbf{s}^c$) of the wheelchair, given all of its sensory inputs, (e.g. the user input, wheel encoders, sonar, laser scanner, camera etc.).

Forming a usable forward model is always a trade–off between the accuracy of the prediction and the complexity of the model. In our case, we disregard some of the peculiarities

of the wheelchair's dynamic response for ease of computation. Most notably, we ignore the effects of the castor wheels, but we also disregard the effects of uneven inclines and changes in coefficients of friction, which can cause wheel slippage [34]. These phenomena most noticeably disturb the physical rotational velocity of the chair when negating the translational velocity commands (resulting in incorrect odometry readings), but not significantly so, when you consider the inevitably inherent errors in the wheelchair sensors. In practice, we have found that the simplified model works sufficiently well to plan safe trajectories, as will be demonstrated in the results section of this paper.

The maximum motor command values are $v_{max}^m = v_{max}^u = 100$ and $\omega_{max}^m = \omega_{max}^u = 100$, which correspond to the full scale deflection (FSD) of the joystick along its vertical and horizontal axes respectively. In this set of experiments, the maximum physical speed of the chair is limited to $v_{max}^c = 1ms^{-1}$ and $\omega_{max}^c = \frac{\pi}{2}rads^{-1}$. We define the coefficient of acceleration to describe how quickly the wheelchair can respond to requests for changes in velocity; this is an inherent property of the dynamics of the wheelchair. We experimentally found it to be $\mathbf{k}_a = \begin{bmatrix} 4 & 4 & 8 \end{bmatrix}^T$, such that the acceleration profile of our model approximately mimics our actual wheelchair. In practice, this means it takes around two seconds to reach maximum speed from standstill.

The wheelchair state transitions are given by:

$$\mathbf{s}_{n+1}^c = \mathbf{s}_n^c + \dot{\mathbf{s}}_n^c T + \mathbf{a}_n^c \frac{T^2}{2}, \tag{14}$$

where $\mathbf{a}_n^c$ is defined as follows. We use the desired velocity signals to accelerate/decelerate the model of the wheelchair until the simulated physical velocities of the chair are equivalent to the desired ones:

$$\mathbf{a}_n^c = \mathbf{k}_a \odot (\boldsymbol{\Gamma} \odot \dot{\mathbf{s}}_n^d - \dot{\mathbf{s}}_n^c), \tag{15}$$

$$\dot{\mathbf{s}}_n^d = \begin{bmatrix} \cos(\theta_n^c) & 0 \\ \sin(\theta_n^c) & 0 \\ 0 & 1 \end{bmatrix} \boldsymbol{\Psi}_n^d. \tag{16}$$

The vector $\boldsymbol{\Gamma}$ is simply the scaling factor that relates the control signals to the desired physical speed of the wheelchair.

$$\boldsymbol{\Gamma} = \begin{bmatrix} \gamma_v & \gamma_v & \gamma_\omega \end{bmatrix}^T, \tag{17}$$

$$\gamma_v = \frac{v_{max}^c}{v_{max}^m}, \qquad \gamma_\omega = \frac{\omega_{max}^c}{\omega_{max}^m}. \tag{18}$$

G. Adaptive Assistance

If the system becomes very confident that a user is aiming for a specific goal, but then their input begins to deviate from the model, some assistance may be required. Alternatively they may have changed their plans; hence the need to adapt the level of assistance based upon the affordances of the surroundings.

Our approach is to gently guide the wheelchair towards the safe mini–trajectory, once we are confident this is where they are headed. Nonetheless, in a manner similar to that of Zeng *et al.* [35], the speed of the manoeuvre is still controlled by the user. The speed is proportional to the component of the amplitude of the joystick signal that falls in the direction

determined by the intelligent controller, in order to follow the safe path. The user is allowed to reverse backwards along the safe path at any time, until the confidence value drops below C_{thresh}, when they revert to *normal* control.

In our implementation, the angular deflection of the joystick from the centre forward position is ξ^u, which can be calculated as:

$$\xi := \arctan\left(\frac{\omega}{v}\right) \qquad (19)$$

We compute a *user gain* coefficient G^u, which indicates the magnitude of the user input in the direction of the computer–generated safe mini–trajectory. This is the coefficient that ensures the user is always in control of the speed of the wheelchair. The larger the discrepancy between the user input and the safe mini–trajectory, the slower the wheelchair will move.

$$G^u = max\left(\frac{\|\mathbf{\Psi}^u\|}{\|\mathbf{\Psi}^u_{max}\|} \cdot \cos(\xi^w - \xi^u), 0\right) \qquad (20)$$

Here, the collaborative controller combines the user input with the control signals generated by the wheelchair's inverse model, based upon the confidence coefficient of the predicted intention.

$$\mathbf{\Psi}^m = \begin{cases} \mathbf{\Psi}^u & \text{if } C \le C_{thresh} \\ G^u\left(C\mathbf{\Psi}^d + (1-C)\mathbf{\Psi}^u\right) & \text{if } C > C_{thresh} \end{cases} \qquad (21)$$

H. Dynamic Local Obstacle Avoidance (DLOA)

There has been much work in the field of mobile robotics with regard to autonomous obstacle avoidance, as reviewed in [36]. Approaches such as the vector field histogram (VFH) [37] are often used. The VFH was later adapted to be used in the context of a powered wheelchair by Levine *et al.* [11]. However, even this extensively modified version was reported to require a minimum of 18 cm of clearance to pass through gaps 70 % of the time, which was not flexible enough for performing our tasks, some of which only allowed 10 cm of clearance. Therefore we took a different approach, similar to the Dynamic Window Approach [29] and Nearness Diagram [38], which is based upon predicting the possible motion of the wheelchair for the following time step. However, since we are not navigating purely autonomously, we can look to the user for a hint and therefore begin the search in the direction indicated by the current user input.

We based our implementation on the forward models that underpin our intention prediction mechanism in the collaborative controller. Using our forward model, we defined the wheelchair's safety zone to be the boundary of the area the wheelchair would traverse in the next 100 ms time-step, plus a velocity-dependent error margin. The zone can include the geometric features of the wheelchair, but it should be noted, that unlike in mobile robots and cars, the users of wheelchairs often have limbs that extend beyond the footprint of the vehicle This safety zone was computed in polar form, as a vector of distances ($\mathbf{Z_w}$) from the centre of the wheelchair, with the index (i) of each element representing the angle (θ) from the heading of the wheelchair, such that:

$$i = \left\lfloor\frac{N_L}{2} + \frac{\theta}{\delta}\right\rfloor, i \in \mathbb{Z}, \qquad (22)$$

Fig. 3. The dynamic local obstacle avoidance (DLOA) algorithm evaluates multiple forward models until it finds the direction that is both safe and closest to the user's intended direction of travel.

Require: $\mathbf{Z_w}$ Wheelchair safety zone
Require: $\mathbf{L}$ Laser range data
Require: N_L Number of laser readings
Require: δ Angular resolution of laser readings
Require: ξ Joystick angle
Require: K_ϵ Maximum angular adjustment (we used $\frac{\pi}{4}$)
  $\phi_0 := \left\lfloor\frac{\xi}{\delta}\right\rfloor$
  $\epsilon := 0$
  repeat
    $\Delta := \phi_0 + \left\lfloor\frac{\epsilon}{2}\right\rfloor$
    safe := **true**
    $i := 0$
    while $i < N_L$ **do**
      $j := i + \Delta$
      if $j \ge 0$ **and** $j < N_L$ **then**
        if $Z_w(j) \ge L(i)$ **then**
          safe := **false**
          break
        end if
      end if
      $i := i + 1$
    end while
    $\epsilon := -\text{sign}(2\epsilon + 1)(|\epsilon| + 1)$
  until safe = **true or** $|\epsilon| > K_\epsilon$
  return $(\text{safe}, \delta\epsilon)$

where N_L is the length of the vector and δ is the angular resolution of our laser scanner.

Next, we evaluate whether or not there were any intersections with the laser range data $\mathbf{L}$, which was also presented as a vector of distances. An intersection would represent a collision, so we must search for a direction to travel that would not result in an intersection and is closest to the user's intended direction. To do this, we constructed the algorithm shown in Fig. 3, which shifts $\mathbf{Z_w}$ — yielding a rotation in Cartesian space — until it finds a suitable direction, or determines there is no safe direction. This process is illustrated in Fig. 4.

Finally, the new motor control signals are generated. If the safe direction that is computed by the DLOA is significantly different to the output from the collaborative control system, the translational velocity is reduced proportionally to this difference and the rotational velocity is set to achieve the newly desired direction, by using the wheelchair's inverse model.

III. METHODOLOGY

The wheelchair platform that we have developed is shown in Fig. 5a. As discussed in the Introduction and in accordance with the recommendations of Tsui *et al.* [39], when evaluating assistive robotic technologies, it is important not only to use traditional robotics metrics, such as speed and accuracy, but also to consider human factors. Therefore, we indirectly measure the user's workload, with the help of a secondary task, whilst we concurrently monitor their visual attention using an eye–tracker (Fig. 5b). Questionnaires are also used to gather feedback from the participants.

It is difficult to recruit large numbers of wheelchair users that are suitable for participating in such experiments, which makes it difficult to provide statistically significant results [40]. Therefore, some research groups have taken the approach of performing an experiment with able–bodied subjects and then
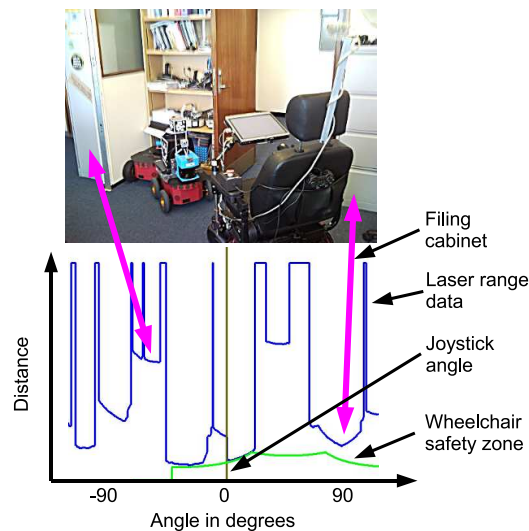
Fig. 4. As the wheelchair faces the gap between the mobile robot and the door, the joystick is set in the straight forward position. However, if the wheelchair's safety zone were centred on the joystick angle, it would intersect with the laser scan. Therefore, the dynamic local obstacle avoidance (DLOA) module shifts it approximately 45 degrees to the right, so that the wheelchair would head towards the open doorway
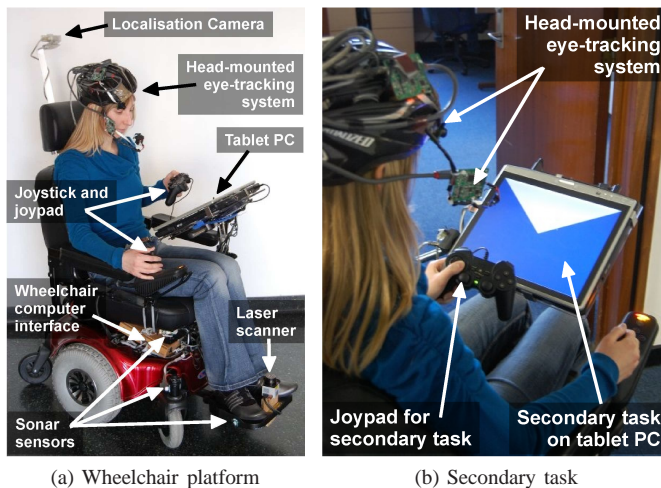

(a) Wheelchair platform   (b) Secondary task

Fig. 5. In this experiment, the user controls the wheelchair with the joystick in their right hand, whilst performing a secondary task on the joypad buttons with their left hand.

documenting a case study with a typical end user [35]. We also use a sample set of able–bodied test subjects and correlate these results with an experimental case study involving an experienced mobility–impaired wheelchair user. We recruited 21 able-bodied volunteers aged between 17 and 47 to participate in the experiments. Each subject took about 40 minutes to complete the trial and fill in a brief questionnaire.

A. Primary Task

Some studies have found that maze–like obstacle courses do not always work well in user evaluations of wheelchairs [39], so we perform our experiments in a real office environment. The primary task involved driving the wheelchair in as safe and effective manner as possible to complete the circuit
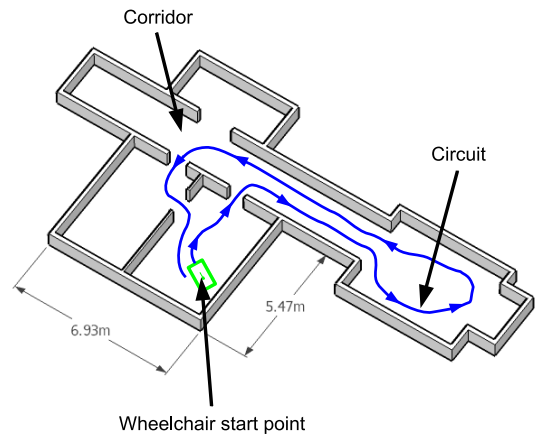

Fig. 6. The primary task was to drive around this circuit in an office environment (the start and finish are at the same location).

shown in Fig. 6. Each lap involved performing manoeuvres in cluttered office environments and navigating a corridor, which resulted in passing through three doorways of varying widths. When the wheelchair passed through the narrowest door, there was only a total of 10 cm in clearance. The ability to navigate through doorways without having a collision is both a common metric that researchers use to evaluate intelligent wheelchairs and a requirement in order to be prescribed a powered wheelchair in some countries [41].

B. Secondary Task

Secondary task reaction times and hit rates are indirect indicators of cognitive workload and have been widely used in driving research [42], [43]. They have not been used extensively in wheelchair research, yet due to the similar nature of the task, we believe they are appropriate and yield compelling evidence. We used the same secondary task as we did in [17], due to the ease of quantitatively measuring the performance and the clear results previously obtained. It was chosen to be deliberately distracting and to require a certain degree of visual attention. This allowed us to determine how users might drive under increased workload.

For the secondary task, the tablet PC screen was coloured dark blue. A single random quadrant of the screen would then be highlighted in white, at random time intervals (bounded between 100 ms and 500 ms), as shown in Fig. 5b. In an effort to obtain a larger volume of reaction data whilst the user was actually driving through the doorways, we set the bound on the time interval to be lower compared with previous experiments [17]. As with the previous set of trials, each participant was told to react as quickly as possible to the quadrant appearing. They had to press the appropriate button on the joypad controller: i.e. the right quadrant of the screen corresponds to the east button on the joypad; the top screen quadrant corresponds to the north button etc.. In the case that a correct button was pressed, the reaction time would be logged, the highlighted quadrant would turn momentarily green, to give the user positive feedback, before reverting back to dark blue and the whole cycle would begin again. Conversely, when an incorrect button had been pressed, the quadrant of

the screen that corresponded to the incorrect button would momentarily turn red (negative feedback) and the secondary task would remain in the same state until the correct button had been pressed.

C. Participant Feedback

At the end of each experiment, the participant was asked to fill in a brief questionnaire about the experience. It was predominantly a comparative questionnaire asking them to indicate how strongly they agreed with each of the statements in Fig. 13, for each control mode, on a five point Likert scale (1 = strongly agreed, 5 = strongly disagreed). Before considering the statements, the participants were told that they only referred to the actual experiment (whilst they were performing the secondary task) not to how they felt during the training periods.

D. Experimental Protocol

First, we calibrated the eye–tracking equipment. The procedure involved the participant focusing sequentially on 9 points of a grid on the computer screen, as described in [18]. The calibration was briefly verified, by checking that the resulting tracked region of interest on the monitor, corresponded with where the participant was actually looking.

The independent variable we were testing was the wheelchair control method, which could take one of two states: provide adaptive assistance, or provide no assistance. To counterbalance any order effects [44], odd numbered participants undertook a set of trials with adaptive assistance before moving on to a set of trials without any assistance. Conversely, even numbered participants undertook the trials without any assistance, before being introduced to the adaptive assistance mode of operation.

Each participant was given five minutes to drive the wheelchair around the office environment and along the corridor, to familiarise themselves with the active control mode. Next, whilst they were stationary, they were introduced to the secondary task (the participants were told this was a *reaction game*). They were then given a practice trial (one lap of the circuit shown in Fig. 6), whilst simultaneously playing the reaction game. It was reiterated that their main task was to drive safely and then to play the reaction game to the best of their ability. They were then asked to repeat the trial, whilst we recorded the experimental data. This was followed by a two minute break before undertaking the entire procedure again for the remaining wheelchair control method (either with adaptive assistance, or without assistance). The second set of trials were identical to the first, apart from the fact that the wheelchair control method was swapped and the stationary practice session of the secondary task was omitted. Each participant therefore performed a total of 4 trials (2 for each condition and we used the 2nd trial of each condition for the data analysis). For safety reasons, we limited the maximum translational velocity of the wheelchair to 1 metre per second and the maximum angular velocity to 90° per second.
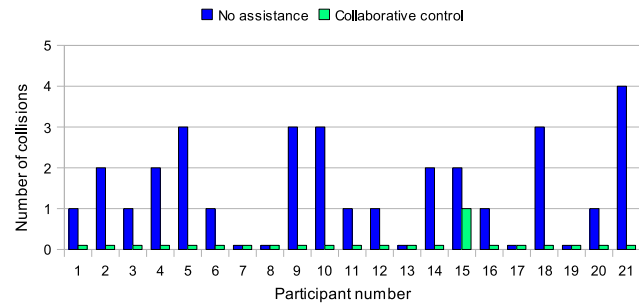

Fig. 7. Number of collisions each user experienced under each condition.

IV. RESULTS

A. Primary Task Results

Perhaps the most safety–critical measure we can use to quantify the performance of the primary task, is to count the number of collisions the participant had during each trial. Two types of collisions were observed: *head–on*, involving the footplate and/or front castors, and *clipping*, which involved the drive wheels or side of the wheelchair. Both types were equally destructive, although head–on collisions generally took longer to recover from, due to re-manoeuvring. Fig. 7 shows that 76% of the participants had at least one collision when they were not given any assistance. Conversely, there was only one collision over all the trials, when the collaborative control method was active and after investigation, this was due to mechanical failure. The bearing–ring had broken on the front right castor, which prevented the wheel from steering. We replaced the bearings before continuing with any further trials.

For safety reasons, the collaborative controller never allows the wheelchair to travel faster than the speed indicated by the user input. This means there is an inherent cost of using the collaborative controller in terms of the time taken to drive a specific course. It took participants an average of 32.6 seconds (SD = 5.2) to complete each run, when not being given any assistance and this increased by an average of 3.7 seconds, when they performed the same task using the collaborative control system. This was also observed in [20], where participants took longer to complete the task using their equivalent of collaborative control, the semi-autonomous mode, compared with the manual and autonomous modes. There is often a trade off between speed and safety from a system point of view and user workload from a human factors point of view.

Since some users required more help than others, a more realistic measure would be the percentage increase in time required for each person to complete the task with the collaborative controller active. In Fig. 8, we show the cost as the percentage increase in the time taken to perform the primary task when using collaborative control, as opposed to being given no assistance. There were a few cases when this cost was negative, meaning the user completed the course more quickly when the collaborative controller was active. In these cases it took longer to complete the course without assistance due to head–on collisions that required the user to reverse before continuing with the primary task.
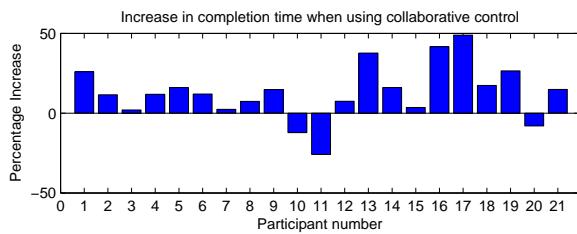
Fig. 8. Only three participants completed the primary task more quickly when assistance was given.
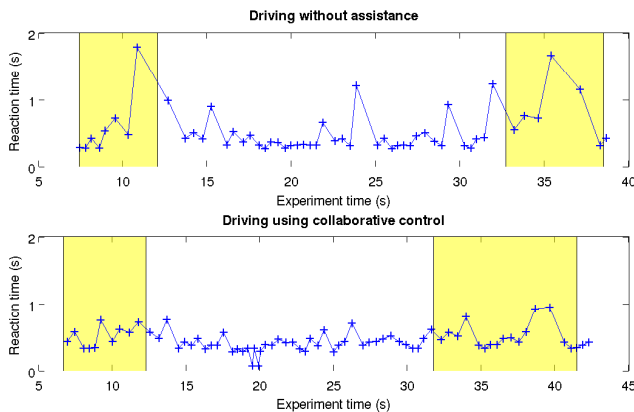

Fig. 9. A comparison of typical secondary task reactions when driving with and without control. In general, a slight increase in reaction times could be observed when negotiating doorways and cluttered spaces, which are indicated by the highlighted regions of the graph.

Furthermore, since we are interested in the effect of collaborative control on human factors, the experimenters carefully observed the behaviour of participants, whilst they were driving. When driving without assistance from the collaborative controller, the experimenters observed many of the participants making rapid corrective joystick movements, which resulted in the chair being driven inefficiently, in a manner akin to bang–bang control [45]. However, this behaviour was not observed when the collaborative controller was active.

We found that this phenomenon could be quantitatively characterised by analysing the joystick signals. The smoothness of movements are typically characterised by the jerk component, which is defined as the third derivative of position, i.e. the rate of change of acceleration [46], [47]. In line with previous studies [16], we found that, when being assisted by the collaborative controller, there was a statistically significant reduction of an average of 23% in the jerk component of the participants' input signals ($p = 0.0015$). This resulted in a much less erratic style of driving. In other studies on shared control, joystick entropy is used, rather than jerk, but similar results were found, albeit with only four participants [48].

B. Secondary Task Results

Typical reaction patterns are shown in Fig. 9 and as we can see in Table I, when not being given any assistance, the mean reaction time increases from 531 ms (SD=0.257) in open spaces to 706 ms (SD=0.518) when negotiating doorways. In open spaces many possible trajectories can be followed with

TABLE I
MEAN REACTION TIMES (SIGNIFICANCE: STUDENT'S t–TEST).

| | Mean reaction times | | |
	Doorways	Elsewhere	*p-value*
No assistance	706ms	531ms	$p = 0.050$
Collaborative control	521ms	470ms	$p = 0.254$
p-value	$p = 0.045$	$p = 0.136$	

little constraint on precision, however the trajectory must be much more precise when manoeuvring through doorways, in order to avoid collisions. Our results indicate that the primary task was more demanding at these points, resulting in a higher cognitive workload [42], [43]. Interestingly, when using the collaborative control method, there was not a corresponding significant increase (for Student's t–test, $p = 0.250$). We can see that compared with when no assistance is given, the collaborative controller has significantly decreased the reaction times from 706 ms (SD=0.518) to 521 ms (SD=0.189) when passing through doorways and cluttered spaces ($p = 0.045$), which suggests the collaborative controller has simplified the navigation task, thus reducing the user's workload.

In keeping with our previous work [17], we find the collaborative controller also significantly decreases the incorrect reactions from 9.2% (SD=4.65) to 6.6% (SD=2.62, $p = 0.032$).

C. Eye–tracking Results

Initially we analysed the eye-tracking video footage manually. Fig. 10 shows some key frames as a participant passes through the doorway without any assistance. In this case, the participant did not check the surroundings in sufficient time to prevent a crash (Fig. 10(c)). Consequently some reversing and re-manoeuvring was required (Fig. 10(d)), before they could focus on the secondary task again. After the crash, the participant appears to take more notice of the surroundings, as shown in Fig. 10(f).

Conversely, when the same participant was assisted by the collaborative controller, there was no need to constantly check the surroundings for obstacles, since the wheelchair would re–align itself, where necessary. In this case, the participant was able to devote much more time to focusing on the secondary task, yet did not have any collisions. Most participants exhibited fairly similar behaviour, spending a larger fraction of their time looking at the secondary task when being given assistance as shown in the histogram of Fig. 12. Some participants did exhibit a slight increase in saccadic eye movements when being assisted on the approach to a doorway. However, on average these increases were not as large as our pilot study suggested [18]. The latest results suggest that when we added the dynamic local obstacle avoidance (DLOA) module, participants became more comfortable with the collaborative system.

To provide a useful quantitative analysis of the eye–tracking results, we calculated both the horizontal and vertical standard deviations of the points of gaze for each subject. The reduction in the standard deviation of points of gaze when being assisted (Fig. 11) correlated strongly with our qualitative observations of the eye movements. On average, when driving with the
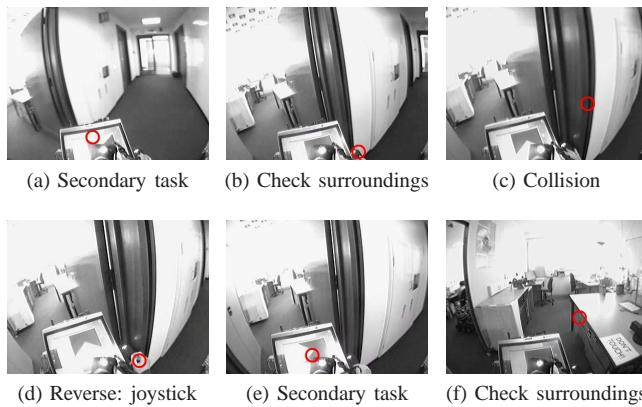
Fig. 10. When no assistance is given a participant crashes into the door–frame. The points of gaze are indicated on the scene images with red circles.
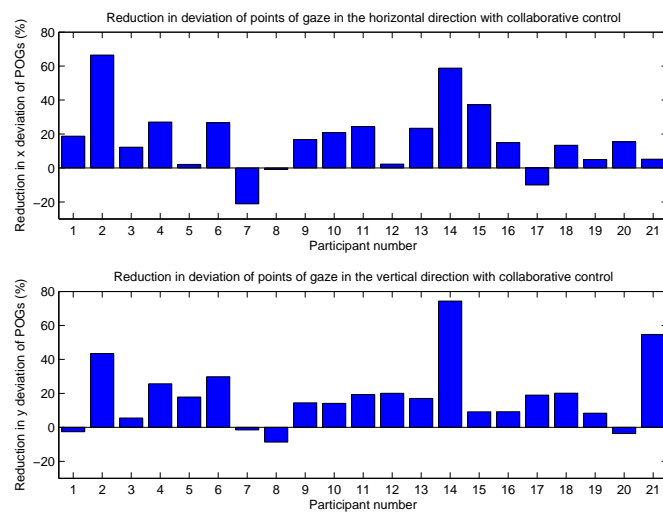
(a) Secondary task (b) Check surroundings (c) Collision
(d) Reverse: joystick (e) Secondary task (f) Check surroundings

Fig. 11. When the participants were assisted by the collaborative controller, there was a statistically significant reduction in eye–movement.

Fig. 12. A histogram showing the percentage of the trial that the user spent looking at different regions of the scene image.

Q1	The wheelchair was easy to manoeuvre.
Q2	The wheelchair behaved as I expected.
Q3	I had to concentrate hard to drive the wheelchair.
Q4	It felt natural driving the wheelchair.
Q5	The reaction game was easy.

Fig. 13. The degree to which participants agreed more strongly (positive values) with each statement when using collaborative control as opposed to being given no assistance.

assistance of the collaborative controller, there was a 15.8% reduction in the standard deviation of the points of gaze in the horizontal direction and an 18.0% reduction in the vertical direction ($p = 0.001$ for both the x and y directions).

D. Questionnaire Results

Each participant indicated how strongly they agreed with each of the statements in Fig. 13 for both sets of trials (i.e. when they were not being given any assistance and when the collaborative controller was active). The results show that on average, people tended to agree that the wheelchair was easy to manoeuvre, behaved as expected, was natural to drive and that the reaction game was easy. They were generally indifferent to the level of concentration required to perform the tasks. However, there was a large standard deviation across the subjects' answers and appeared to be little difference between the perceptions of the system when using the collaborative controller compared with when no assistance was given.

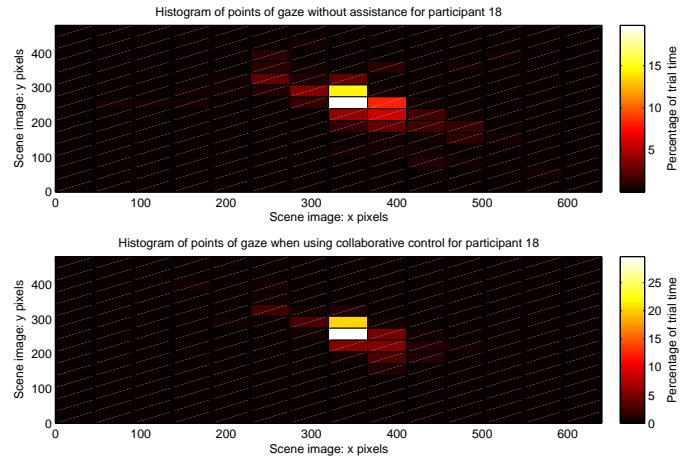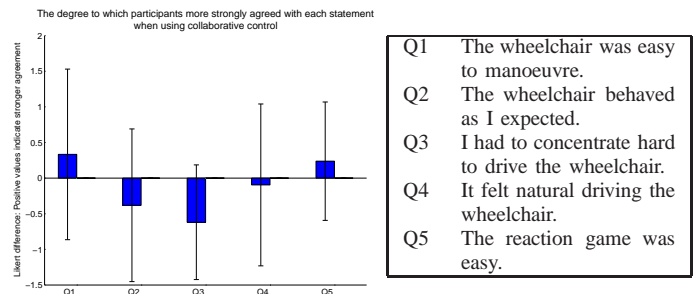When doing a between subjects analysis of the results, we found no statistically significant trends, meaning that what some people found *easy* or *natural*, others did not. Since each participant has their own personal expectations and subjective opinions of whether a task was *easy* or not, much like they have their own thresholds of pain [49], we therefore decided to do a within subjects analysis.

Using the same questionnaire data, we compared the Likert ranking of each statement for the case when assistance was given with that when no assistance was given, for each individual participant. The graph in Fig. 13, shows how much more strongly participants agreed with each statement, when using collaborative control. The only question that showed a statistically significant response ($p = 0.003$) was that people agreed more strongly with the statement "I had to concentrate hard to drive the wheelchair", when they were *not* being assisted by the collaborative controller.

V. CASE STUDY

The quantitative data presented so far has related to trials with able–bodied subjects. In this section, we compare these results with those obtained from a trial with a wheelchair user. The volunteer participant suffers from complex regional pain syndrome (CRPS) and arthritis. This means that she cannot put any pressure on her left leg and has difficulty using crutches because of the complex nature of her condition. To increase her independence, she uses a manual wheelchair to get around

TABLE II
QUESTIONNAIRE RESPONSES FROM A WHEELCHAIR USER (LIKERT
VALUES 1 = STRONG AGREEMENT, 5 = STRONG DISAGREEMENT)

	Statement Number				
	Q1	Q2	Q3	Q4	Q5
No assistance	2	4	5	2	2
Collaborative control	1	4	5	1	1

TABLE III
MEAN REACTION TIMES FOR AN EXPERIENCED WHEELCHAIR USER

	Mean reaction times		
	Doorways	Elsewhere	*p-value*
No assistance	860ms	1032ms	$p = 0.081$
Collaborative control	583ms	541ms	$p = 0.914$
p-value	$p = 0.033$	$p = 0.013$	

Fig. 14. An experienced wheelchair user's pattern of reactions. Doorways and cluttered spaces are highlighted.

without exacerbating her joint pains. However, she finds it very tiring to propel herself manually for more than an hour or so. Therefore, when she is shopping or travelling further afield, she prefers to use a powered wheelchair. When performing the trials with the wheelchair user, we followed exactly the same protocol that we had previously used with healthy subjects (as described in Section III-D).

A. Experimental Results for a Wheelchair User

The responses given to our questionnaire are recorded in Table II. It was contrary to our experienced wheelchair user's expectations that whilst performing the secondary task, she found it easier to manoeuvre with assistance from the collaborative controller. Despite this, the wheelchair did not behave as she expected in either trial; predominantly due to the dynamics of the chair being quite different from her own wheelchair [50]. In particular, to increase safety, the chair had been speed–limited and sudden changes of direction were not permitted (these parameters are often be set by the wheelchair provider, when a user is assessed for a wheelchair [1]).

The participant perceived the reaction game to be easier to play when she was driving with assistance from the collaborative controller. This correlates well with her increase in secondary task performance: when not driving through doorways, her reactions times almost halved from 1032 ms to 541 ms (Table III).

When being assisted by the collaborative controller, the standard deviation of the participant's points of gaze reduced more significantly than those of the able–bodied participants. Averaged across her trials, it reduced by 41.1% in the horizontal direction and 45.7% in the vertical direction. We hypothesise that this is because, being an experienced wheelchair user, she is more aware of potential obstacles (including pedestrians) than inexperienced users. However, throughout the training period she became more accustomed to the collaborative system. In her trials, she left the collision avoidance and heading correction to the wheelchair, allowing her to pay more attention to the secondary task.

The improvement in the percentage of incorrect reactions was not found to be statistically significant on its own ($p = 0.185$), due to the limited number of trials we were able to run. However, it does mimic the results obtained from our able–bodied participants, with the mean percentage of
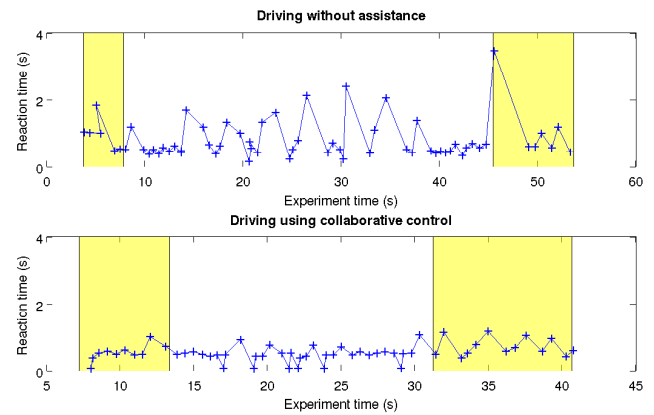
incorrect reactions when using collaborative control (8.9%) falling within the standard deviation of the results obtained in Section IV-B. Moreover the percentage of reactions that were incorrect when no assistance was given was even higher than our previous findings with able–bodied participants.

Whilst performing the experiment without being given assistance, the wheelchair user experienced two minor crashes. The first occurred when she was focused on the secondary task and tried to turn right too early as she was coming out of a doorway into the corridor. This meant that the driving wheels caught on the door–frame. The second time was a left turn, entering a different office from the corridor. This time having been travelling relatively fast down the corridor whilst paying little attention to her driving, she approached the doorway at speed and slightly overshot it, bumping the footplate into the door–frame. In both of these cases, she had to reverse and re-align the wheelchair, in order to successfully complete the circuit; this added to her primary task completion time.

Conversely, when the collaborative controller was active, similar crashes were prevented by not letting the chair turn, until it was clear of an obstacle (or door–frame). Additionally, if the chair was approaching a narrow gap, it would proactively slow down and align to the gap, which prevented overshooting doorways, even if the initial approach was at relatively high speed. Additionally, we observed a change in the wheelchair user's behaviour in terms of the manipulation of the joystick, which correlated with that of the healthy participants (see Section IV-A). When being assisted by the collaborative controller, the jerk component in the joystick signals reduced by 34%, which resulted in visibly smoother hand movements and consequently more efficient trajectories.

Although on average the wheelchair user did complete the primary driving task marginally more quickly when using the collaborative controller, her results do not statistically significantly contradict our findings with able bodied subjects. Both her mean completion times fell within the standard deviation of our experiments with able-bodied participants ($p = 0.620$). The main reason that her task completion times deteriorated when driving without assistance was due to her needing to reverse and correct the trajectory after the collisions, which

occurred in each of her non-assisted trials.

B. A Qualitative Analysis of the Collaborative Controller

When choosing a new wheelchair, the end user is encouraged to "test drive the new model in the real world, just as one would test drive a new car on the roads" [50]. Therefore, in addition to gaining the quantitative data from the wheelchair user's experiments, she agreed to assess the wheelchair from a user's perspective. The main advantages of our system that she identified, was that it did proactively help with the steering (preventing collisions), but at the same time allowed her to get close enough to objects to interact with them. In particular, she managed to help herself to a drink from the water cooler.

However, she did feel some points should be addressed. She found it sometimes "overcompensated" when a collision was predicted; this was because safety was our primary concern. However, the sensitivity of the system could be reduced, particularly through the use of long–term learning and user–modelling techniques [51]. Additionally, she found that the chair could not detect overhanging tabletops. It is difficult to reliably detect a table, since a planar laser scanner is insufficient and sonar sensors by themselves are not reliable [52]. It may be possible to solve the problem, using other devices such as stereo or infrared time–of–flight cameras [53], however, reliable sensors and techniques to do this currently remain an open area of research.

VI. Conclusion

We have comprehensively evaluated our shared control system, placing particular emphasis on the human factors analysis. A suit of tools, including: joystick signal analysis, secondary tasks and eye-tracking has yielded statistically significant results from 21 healthy subjects. We have shown that our collaborative control mechanisms have enabled people to drive the wheelchair safely, at a slight cost in time, whilst concurrently reducing the demands on visual attention, cognitive workload and manual dexterity. Furthermore, we have found that even an experienced wheelchair user who is mobility impaired, but still able to operate a joystick with a reasonable degree of precision, can benefit from shared control under specific circumstances, i.e. when under a heightened workload or inattentive to the task.

VII. Future work and further applications

People with severe physical disabilities may not be able to interact through conventional interfaces and instead may benefit from solutions such as brain–computer interfaces (BCI) [8]. However, it is difficult to control a powered wheelchair safely and efficiently, using the BCI directly, due to the low information rate [54]. We have shown how safe and efficient manoeuvres can be achieved, even when there is a lack of precision in the user's input. Therefore, collaborative control may be the key to compensating for this in BCIs. Moreover, initial work with a tele–operated robot has shown that a shared control paradigm has reduced the number of BCI commands required to follow a specified trajectory [55], which is akin to our findings whereby using collaborative control resulted in a reduced amount of joystick movement [16].

References

[1] D. Sanderson, M. Place, and D. Wright, "Evaluation of the powered wheelchair and voucher scheme initiatives," NHS Executive and Department of Health: York Health Economics Consortium, The University of York (UK), Tech. Rep., March 2000.

[2] R. Simpson, D. Poirot, and F. Baxter, "The hephaestus smart wheelchair system," *IEEE Transactions on Neural Systems and Rehabilitation Engineering*, vol. 10, no. 2, pp. 118–122, June 2002.

[3] S. Evans, C. Neophytou, L. D. Souza, and A. O. Frank, "Young people's experiences using electric powered indoor - outdoor wheelchairs (epiocs): potential for enhancing users' development?" *Disability and Rehabilitation*, vol. 29, no. 16, pp. 1281–1294, August 2007.

[4] A. Frank, J. Ward, N. Orwell, C. McCullagh, and M. Belcher, "Introduction of a new nhs electric-powered indoor/outdoor chair (epioc) service: benefits, risks and implications for prescribers," *Clinical Rehabilitation*, no. 14, pp. 665–673, 2000.

[5] R. Cooper, M. Boninger, D. Spaeth, D. S. G. Ding, A. Koontz, S. Fitzgerald, R. Cooper, A. Kelleher, and D. Collins, "Engineering better wheelchairs to enhance community participation," *Neural Systems and Rehabilitation Engineering, IEEE Transactions on*, vol. 14, no. 4, pp. 438–455, Dec. 2006.

[6] T. Taha, J. Miro, and G. Dissanayake, "POMDP-based long-term user intention prediction for wheelchair navigation," in *Proceedings of IEEE International Conference on Robotics and Automation (ICRA)*, Pasadena, LA, May 2008, pp. 3920–3925.

[7] Q. Zeng, B. Rebsamen, E. Burdet, and Chee Leong Teo, "A collaborative wheelchair system," *IEEE Transactions on Neural Systems and Rehabilitation Engineering*, vol. 16, no. 2, pp. 161–170, April 2008.

[8] J. del R. Millán, F. Renkens, J. Mouriño, and W. Gerstner, "Noninvasive brain-actuated control of a mobile robot by human EEG," *Proceedings of IEEE Transactions on Biomedical Engineering*, vol. 51, no. 6, pp. 1026–1033, June 2004.

[9] R. Simpson and S. Levine, "Voice control of a powered wheelchair," *IEEE Transactions on Neural Systems and Rehabilitation Engineering*, vol. 10, no. 2, pp. 122–125, June 2002.

[10] H. A. Yanco, *Assistive Technology and Artificial Intelligence*, ser. Lecture Notes in Computer Science.   Springer Berlin / Heidelberg, 1998, vol. 1458, ch. Wheelesley: A robotic wheelchair system: Indoor navigation and user interface, pp. 256–268.

[11] S. Levine, D. Bell, L. Jaros, R. Simpson, Y. Koren, and J. Borenstein, "The navchair assistive wheelchair navigation system," *IEEE Transactions on Rehabilitation Engineering*, vol. 7, no. 6, 1999.

[12] D. Ding and R. A. Cooper, "Electric powered wheelchairs: A review of current technology and insight into future directions," *IEEE Control Systems Magazine*, vol. 25, no. 2, pp. 22–34, April 2005.

[13] T. Carlson and Y. Demiris, "Human-wheelchair collaboration through prediction of intention and adaptive assistance," in *Proceedings of IEEE International Conference on Robotics and Automation (ICRA)*, Pasadena, CA, 2008, pp. 3926–3931.

[14] P. Nisbet, "Who's intelligent? Wheelchair, driver or both?" in *Proceedings IEEE International Conference on Control Applications*, Glasgow, Scotland, U.K., September 2002.

[15] Å. Brandt, S. Iwarsson, and A. Ståhle, "Older people's use of powered wheelchairs for activity and participation," *Journal of Rehabilitation Medicine*, vol. 36, no. 2, pp. 70–77, 2004.

[16] T. Carlson and Y. Demiris, "Collaborative control in human wheelchair interaction reduces the need for dexterity in precise manoeuvres," in *Proceedings of Robotic Helpers: User Interaction, Interfaces and Companions in Assistive and Therapy Robotics, a Workshop at ACM/IEEE HRI 2008*, Amsterdam, The Netherlands, March 2008, pp. 59–66.

[17] ——, "Increasing robotic wheelchair safety with collaborative control: Evidence from secondary task experiments," in *Proceedings of IEEE International Conference on Robotics and Automation (ICRA)*, Anchorage, Alaska, May 2010, pp. 5582–5587.

[18] ——, "Using visual attention to evaluate collaborative control architectures for human robot interaction," in *Proceedings of New Frontiers in Human Robot Interaction, a symposium at AISB 2009*, Edinburgh, UK, April 2009, pp. 38–43.

[19] L. Montesano, M. Diaz, S. Bhaskar, and J. Minguez, "Towards an intelligent wheelchair system for users with cerebral palsy," *Neural Systems and Rehabilitation Engineering, IEEE Transactions on*, vol. 18, no. 2, pp. 193–202, april 2010.

[20] S. Parikh, V. J. Grassi, V. Kumar, and J. Jun Okamoto, "Usability study of a control framework for an intelligent wheelchair," in *Proceedings of IEEE International Conference on Robotics and Automation (ICRA)*, Barcelona, Spain, April 2005, pp. 4745–4750.

[21] J. Philips, J. del R. Millán, G. Vanacker, E. Lew, F. Galán, P. W. Ferrez, H. V. Brussel, and M. Nuttin, "Adaptive shared control of a brain-actuated simulated wheelchair," in *Proceedings of the 2007 IEEE 10th International Conference on Rehabilitation Robotics*, Noordwijk, The Netherlands, June 12-15 2007, pp. 408–414.

[22] M. Kalkusch, T. Lidy, N. Knapp, G. Reitmayr, H. Kaufmann, and D. Schmalstieg, "Structured visual markers for indoor pathfinding," in *Proceedings of The First IEEE International Workshop on the Augmented Reality Toolkit*, 2002.

[23] W. Burgard, D. Fox, and S. Thrun, "Active mobile robot localization," in *International Joint Conference on Artificial Intelligence*, 1997, pp. 1346–1352.

[24] J.-A. Meyer and D. Filliat, "Map-based navigation in mobile robots:: II. a review of map-learning and path-planning strategies," *Cognitive Systems Research*, vol. 4, no. 4, pp. 283–317, December 2003.

[25] Y. Demiris, "Prediction of intent in robotics and multi-agent systems," *Cognitive Processing*, vol. 8, no. 3, September 2007.

[26] S. Carberry, "Techniques for plan recognition," *User Modeling and User-Adapted Interaction: The Journal of Personalization Research*, vol. 11, no. 1-2, pp. 31–48, 2001.

[27] Y. Demiris and B. Khadhouri, "Hierarchical attentive multiple models for execution and recognition of actions," *Robotics and Autonomous Systems*, vol. 54, pp. 361–369, 2006.

[28] I. Ulrich and J. Borenstein, "Vfh+: reliable obstacle avoidance for fast mobile robots," in *Proceedings of IEEE International Conference on Robotics and Automation*, vol. 2, May 1998, pp. 1572–1577.

[29] D. Fox, W. Burgard, and S. Thrun, "The dynamic window approach to collision avoidance," *Robotics Automation Magazine, IEEE*, vol. 4, no. 1, pp. 23–33, mar 1997.

[30] S. Quinlan and O. Khatib, "Elastic bands: connecting path planning and control," in *In proceedings of the IEEE International Conference on Robotics and Automation*, 1993, pp. 802–807.

[31] P. Morin and C. Samson, "Motion control of wheeled mobile robots," in *Springer Handbook of Robotics*, B. Siciliano and O. Khatib, Eds. Springer Berlin Heidelberg, 2008, pp. 799–826.

[32] R. Siegwart and I. Nourbakhsh, *Introduction to Autonomous Mobile Robots*. Cambridge, MA: MIT Press, 2004.

[33] G. F. Franklin, J. D. Powell, and A. Emami-Naeini, *Feedback Control of Dynamic Systems*. Addison–Wesley, 1986.

[34] C. Ward and K. Iagnemma, "Model-based wheel slip detection for outdoor mobile robots," in *Proceedings of IEEE International Conference on Robotics and Automation (ICRA)*, April 2007, pp. 2724–2729.

[35] Q. Zeng, E. Burdet, B. Rebsamen, and C. L. Teo, "Evaluation of the collaborative wheelchair assistant system," in *Proceedings of IEEE Conference on Rehabilitation Robotics*, The Netherlands, June 2007.

[36] J. Minguez, F. Lamiraux, and J.-P. Laumond, "Motion planning and obstacle avoidance," in *Springer Handbook of Robotics*, B. Siciliano and O. Khatib, Eds. Springer Berlin Heidelberg, 2008, pp. 827–852.

[37] J. Borenstein and Y. Koren, "The vector field histogram - fast obstacle avoidance for mobile robots," *IEEE Transactions on Robotics and Automation*, vol. 7, no. 3, pp. 278–288, 1991.

[38] J. Minguez and L. Montano, "Nearness diagram (nd) navigation: collision avoidance in troublesome scenarios," *Robotics and Automation, IEEE Transactions on*, vol. 20, no. 1, pp. 45–59, february 2004.

[39] K. Tsui, H. Yanco, D. J. Feil-Seifer, and M. J. Matarić, "Survey of domain-specific performance measures in assistive robotic technology," in *Proceedings of the Performance Metrics for Intelligent Systems Workshop*, Washington, D.C., Aug 2008, pp. 116–123.

[40] H. A. Yanco, "Shared user-computer control of a robotic wheelchair system," Ph.D. dissertation, Massachusetts Institute of Technology, 2000.

[41] K. M. Tsui, D. J. Feil-Seifer, M. J. Matarić, and H. A. Yanco, "Performance evaluation methods for assistive robotic technology," in *Performance Evaluation and Benchmarking of Intelligent Systems*, R. Madhavan, E. Tunstel, and E. Messina, Eds. Springer US, 2009, pp. 41–66.

[42] C. J. D. Patten, A. Kircher, J. Östlund, and L. Nilsson, "Using mobile telephones: cognitive workload and attention resource allocation," *Accident Analysis & Prevention*, vol. 36, no. 3, pp. 341–350, 2004.

[43] D. Crundall, G. Underwood, and P. Chapman, "Driving experience and the functional field of view," *Perception*, vol. 28, pp. 1075–1087, 1999.

[44] H. Coolican, *Research methods and statistics in psychology*, 2nd ed. Hodder & Stoughton, 1994.

[45] R. J. Jagacinski and J. Flach, *Control theory for humans: quantitative approaches to modeling performance*. Laurence Erlbaum Associates, 2003.

[46] T. Flash and N. Hogan, "The coordination of arm movements: an experimentally confirmed mathematical model," *Journal of Neuroscience*, vol. 5, no. 7, pp. 1688–1703, 1985.

[47] D. Liu and E. Todorov, "Evidence for the flexible sensorimotor strategies predicted by optimal feedback control," *Journal of Neuroscience*, vol. 27, no. 35, pp. 9354–9368, 2007.

[48] J. W. Crandall and M. A. Goodrich, "Characterizing efficiency of human robot interaction: A case study of shared-control teleoperation," in *Proceedings of the 2002 IEEE/RSJ International Conference on Intelligent Robots and Systems*, Lausanne, Switzerland, 2002, pp. 1290–1295.

[49] J. D. Hardy, H. G. Wolff, and H. Goodell, "Studies on pain. a new method for measuring pain threshold: Observations on spatial summation of pain," *The Journal of Clinical Investigation*, vol. 19, no. 4, pp. 649–657, July 1940.

[50] M. Batavia, A. I. Batavia, and R. Friedman, "Changing chairs: anticipating problems in prescribing wheelchairs," *Disability & Rehabilitation*, vol. 23, no. 12, pp. 539–548, 2001.

[51] Y. Demiris and T. Carlson, "Lifelong robot-assisted mobility: models, tools, and challenges," *IET Seminar Digests*, vol. 2009, no. 12725, pp. 7–7, 2009.

[52] T. Dutta and G. Fernie, "Utilization of ultrasound sensors for anti-collision systems of powered wheelchairs," *IEEE Transactions on Neural Systems and Rehabilitation Engineering*, vol. 13, no. 1, pp. 24–32, March 2005.

[53] A. Mihailidis, P. Elinas, J. Boger, and J. Hoey, "An intelligent powered wheelchair to enable mobility of cognitively impaired older adults: An anticollision system," *IEEE Transactions on Neural Systems and Rehabilitation Engineering*, vol. 15, no. 1, pp. 136–143, March 2007.

[54] J. del R. Millán and J. Carmena, "Invasive or non-invasive: understanding brain–machine interface technology," *IEEE Engineering in Medicine and Biology Magazine*, vol. 29, no. 1, pp. 16–22, 2010.

[55] L. Tonin, R. Leeb, M. Tavella, S. Perdikis, and J. del R. Millán, "The role of shared-control in bci-based telepresence," in *In proceedings of the IEEE International Conference on Systems, Man and Cybernetics*, 2010, pp. 1462–1466.

Tom Carlson received the M.Eng. (2006) in Electronic Engineering and the Ph.D. (2010) in Intelligent Robotics, under the supervision of Dr. Yiannis Demiris at Imperial College London.

He is currently pursuing post–doctoral research in shared control for brain machine interfaces (BMI) at the École Polytechnique Fédérale de Lausanne (EPFL). His primary research interests include human robot interaction, shared control and robotic assistive devices.

Yiannis Demiris is a senior lecturer in Human-Robot Interaction at the Department of Electrical and Electronic Engineering at Imperial College London, where he heads the Biologically Inspired Assistive Robots and Teams lab (BioART).

His research interests include biologically inspired robotics, human-robot interaction, developmental robotics, and robotic assistive devices.